

The HST Survey of BL Lacertae Objects. IV. Infrared Imaging of Host Galaxies

Riccardo Scarpa, C. Megan Urry, Paolo Padovani¹, Daniela Calzetti & Matthew O'Dowd
Space Telescope Science Institute

ABSTRACT

The HST NICMOS Camera 2 was used for H-band imaging of 12 BL Lacertae objects taken from the larger sample observed with the WFPC2 in the R band (Urry et al. 2000; Scarpa et al. 2000). Ten of the 12 BL Lacs are clearly resolved, and the detected host galaxies are large, bright ellipticals with average absolute magnitude $\langle M_H \rangle = -26.2 \pm 0.45$ mag and effective radius $\langle r_e \rangle = 10 \pm 5$ kpc. The rest-frame integrated color of the host galaxies is on average $\langle R-H \rangle = 2.3 \pm 0.3$, consistent with the value for both radio galaxies and normal, non-active elliptical galaxies, and indicating the dominant stellar population is old. The host galaxies tend to be bluer in their outer regions than in their cores, with average color gradient $\Delta(R-H)/\Delta \log r = -0.2$ mag, again consistent with results for normal non-active elliptical galaxies. The infrared Kormendy relation, derived for the first time for BL Lac host galaxies, is $\mu_e = 3.8 \log r_e + 14.8$, fully in agreement with the relation for normal ellipticals. The close similarity between BL Lac host galaxies and normal ellipticals suggests the active nucleus has surprisingly little effect on the host galaxy. This supports a picture in which all elliptical galaxies harbor black holes which can be actively accreting for some fraction of their lifetime.

Subject Headings: BL Lacertae objects — galaxies: structure — galaxies: elliptical

1. Introduction

The properties of BL Lac host galaxies have been the subject of intense study. Early work from the ground found that nearby BL Lacertae objects were surrounded by luminous elliptical galaxies (Ulrich 1989 and reference therein). With higher resolution

¹Also affiliated to the Astrophysics Division, Space Science Department, European Space Agency, on leave from Dipartimento di Fisica, II Università di Roma “Tor Vergata”.

ground-based observations (Abraham et al. 1991; Stickel et al. 1993; Wurtz, Stocke & Yee 1996; Kotilainen, Falomo & Scarpa 1998a; Falomo & Kotilainen 1999), and now with the 0.1-arcsecond spatial resolution of the Hubble Space Telescope (HST) (Jannuzi, Yanny & Impey 1997; Yanny, Jannuzi & Impey 1997; Falomo et al. 1997; Urry et al. 2000; Scarpa et al. 2000), this result has been extended to much higher redshifts. Detection and morphological classification of BL Lac host galaxies is now almost routine for redshifts $z \lesssim 0.5$.

Nearly 100 BL Lac host galaxies have been detected so far, and there is now abundant evidence that most, and possibly all, BL Lac host galaxies are ellipticals (Abraham et al. 1991; Wurtz et al. 1996; Scarpa et al. 2000). Although there have been claims of spiral structure in a few host galaxies (Abraham et al. 1991; Wurtz et al. 1996), our HST survey of 110 BL Lac objects found overwhelming preference for $r^{1/4}$ -law surface brightness profiles, and no cases where an exponential disk profile was preferred (Falomo et al. 1997; Urry et al. 2000; Scarpa et al. 2000). Given this large sample, the fraction of spiral galaxies among BL Lac hosts must be less than 7% at the 99% confidence level (Scarpa et al. 2000). This holds for both radio- and X-ray-selected BL Lac objects, and can be extended (though with less accuracy) to the more powerful flat spectrum radio quasars (Kotilainen, Falomo & Scarpa 1998b).

With high-resolution images in multiple filters, it is possible to probe the stellar populations of AGN host galaxies, and to compare them to normal ellipticals. Indeed, since many normal (non-active) galaxies appear to have central super-massive black holes (Richstone et al. 1998, van der Marel 1999), perhaps all elliptical galaxies have the potential to become active when accretion is turned on. If so, the stellar populations of AGN host galaxies should be the same as those of normal ellipticals.

Integrated colors and color profiles have been reported for a handful of BL Lac host galaxies (Urry et al. 1999; Kotilainen, Falomo & Scarpa 1998a). These sparse data suggest that BL Lac host galaxies are not strongly affected by the intense activity at their centers, a result with obvious implications for the galaxy-AGN connection, and galaxy and AGN evolution.

To further investigate the colors of BL Lac host galaxies, we observed 12 BL Lac objects in the H-band with the HST² Near-Infrared Camera and Multi-Object Spectrometer (NICMOS). The targets were taken from the larger sample studied previously in the R

²Based on observations made with the NASA/ESA Hubble Space Telescope, obtained at the Space Telescope Science Institute, which is operated by the Association of Universities for Research in Astronomy, Inc., under NASA contract NAS 5-26555.

band with the HST Wide Field and Planetary Camera 2 (WFPC2). For these 12 BL Lac objects we therefore have high-resolution HST observations in two filters probing rather long wavelengths, where the bulk of the emission of the old stellar population lies. These data allow us to derive color profiles and integrated galaxy colors which constrain the stellar content of these host galaxies. The observed sources cover the redshift range $0.1 < z < 0.5$, at the upper end of which cosmic evolution begins to have an effect.

In Section 2 we describe the NICMOS observations and data analysis, Section 3 gives the results and discusses them, Section 4 is discussion and conclusions. Throughout the paper we use $H_0 = 50 \text{ km/s/Mpc}$ and $q_0 = 0$.

2. Observations and Data Reduction

The HST NICMOS Camera 2 was used to obtain high resolution images of 12 BL Lac objects in snapshot mode (that is, during random gaps in the HST observing schedule). The approved list of targets consisted of 29 BL Lac objects from our original WFPC2 snapshot survey list of 132 BL Lacs, comprising seven complete, flux-limited samples selected in the radio, optical, or X-ray. The 29 NICMOS targets had existing WFPC2 F702W data, were uniformly distributed in the redshift range $0.1 < z < 0.5$, and include both “red” (low-frequency-peaked, high-power) and “blue” (high-frequency-peaked, low-power) BL Lac jets (Urry 1999). In the end, data were obtained for 8 blue and 4 red BL Lacs. Among them is 0454+844, for which a corrected redshift, $z > 1.3$, was subsequently reported.

Observations were made in the F160W filter, which has $\lambda_{eff} = 1.6\mu\text{m}$ and closely matches the standard H-band. Camera 2 has pixel size 0.075 arcsec, providing at $1.6 \mu\text{m}$ Point Spread Function (PSF) sampling as good as the WFPC2 planetary camera (which has pixel size of 0.046 arcsec) in the R-band. For each BL Lac, we obtained three separate images with increasing exposure times, dithered to improve resolution and to better estimate sky background. The journal of observations is given in Table 1.

Data were first reduced and flux calibrated in the standard HST pipeline. The effect of the random bias (known as the “pedestal”) was then removed as follows: first, all detected sources in the field of view were excluded; then, considering each of four quadrants separately, we found the value of the pedestal that minimized the spread in the remaining (non-source) pixels, with the added constraint that the sky background had to be the same in all four quadrants. Corrected images were then cleaned of cosmic rays and other defects, and a sky frame (obtained from median filtering the three images) was subtracted. To improve the resolution and PSF sampling in the final combined image we then re-sampled

each image, splitting each pixel into four sub-pixels. These re-sampled images were re-centered matching the peak of the BL Lac light centroid to within 0.2 pixels, and then combined. The final images are presented as contour plots in Figure 1.

The azimuthally averaged, surface brightness radial profiles, shown in Figure 2, were fitted following the same procedure outlined by Scarpa et al. (2000), which is based on a χ^2 minimization strategy. To model the PSF we used the Tiny Tim software (Krist 1995). For the two unresolved sources in our sample (0851+202 and 0454+884), the Tiny Tim PSF model follows the azimuthally averaged surface brightness profile to at least 3.5 arcsec from the nucleus (see Fig. 2), showing it correctly describes the true PSF. In 9 of the other 10 sources, the observed radial profile lies significantly above the PSF model, leaving no doubt that the host galaxy is detected. In the tenth case, 1749+096, the host galaxy is marginally detected; however, the host galaxy was clearly detected in our WFPC2 F702W image (Scarpa et al. 2000) and modeling the excess of light above the Tiny Tim PSF we obtain for the host galaxy a R-H color consistent with the value expected for a normal elliptical galaxy ($R - H = 2.3$ at $z = 0.32$). Thus we conclude that 1749+096 is resolved and that the Tiny Tim software models the NICMOS Camera 2 PSF very well.

3. Results and Discussion

3.1. Morphology and Luminosity of the Host Galaxies

Snapshot images are typically shorter than would be ideal for studying extended emission from the host galaxy. Therefore rather than using a full two dimensional approach, we chose to extract azimuthally averaged radial profiles, which can be traced out to ~ 3 –4 arcsec from the center (Fig. 2), significantly increasing the signal-to-noise and providing well-constrained total magnitude and effective radius for the host galaxies, at the expenses of some spatial information like ellipticity and position angle. From the two-dimensional analysis of the R-band data of all $z < 0.2$ sources observed in the optical survey, which included 5 of the 12 objects presented here, we know that BL Lac host galaxies are quite round and have undisturbed morphology (Falomo et al. 2000). Thus, we are confident that our one-dimensional approach is not biased or affected by unusual feature of the host galaxy.

Ten of the 12 observed BL Lac objects are clearly resolved in the NICMOS images. The two unresolved BL Lacs are the distant source 0454+844 ($z > 1.3$), and 0851+202 (OJ 287, $z = 0.306$), which has a very luminous nucleus and has so far resisted all attempts to resolve its host galaxy (see Yanny, Jannuzi & Impey 1997 and counter arguments by

Sillanpää et al. 1998).

The average radial profiles are in all cases well described by a PSF plus a de Vaucouleurs ($r^{1/4}$) law (Figure 2). In no case is a disk galaxy preferred (for 0502+675 and 1749+096 the two galaxy models are equally acceptable.) The average extinction and K-corrected absolute H magnitude of the 10 resolved hosts is $\langle M_H \rangle = -26.2 \pm 0.45$ mag (standard deviation).

The average effective radius is $\langle r_e \rangle = 10 \pm 5$ kpc, and it ranges from 3 to 20 kpc. The derived magnitudes and effective radii are given in Table 2. These results fully confirm what was found from the R-band HST images, that the host galaxies are giant ellipticals, on average ~ 1 mag brighter than an M^* galaxy ($M_H^* = -25.0 \pm 0.3$ mag; Mobasher, Sharples & Ellis 1993).

3.2. Host Galaxy Integrated Color

The extinction-corrected host galaxy total magnitudes, derived from the best fit de Vaucouleurs model allow us to derive integrated R–H colors for all 10 resolved sources (R-band data are in Table 2 of Urry et al. 2000). Results, summarized in Table 3, show that the average BL Lac host galaxy color is $R-H=2.3 \pm 0.3$ mag, consistent with the value 2.2 ± 0.5 found for 5 more BL Lac objects by Kotilainen, Falomo & Scarpa (1998a), as well as with the value reported for a sample of 12 nearby normal elliptical galaxies, $R-H=2.3 \pm 0.2$ mag (Peletier et al. 1990; value converted from V–K assuming $V-R=0.58$ and $H-K=0.22$, according to Recilla-Cruz et al. 1990).

In the top panel of Figure 3 we plot the R–H colors of our BL Lac host galaxies, computed from extinction and K-corrected magnitudes derived from our WFPC2 and NICMOS data. (In the absence of evolution, the K correction removes the dependence of color on redshift). The BL Lac host galaxy colors cluster around the average color of normal, $z = 0$ galaxies (dashed line in Fig. 3).

We now compare the BL Lac host galaxies to radio galaxies for which infrared colors are available. From the work of Lilly and Longair (1982), eight 3C radio galaxies (3C33, 98, 123, 192, 219, 295, 299, and 388) have measured R–K colors, $z < 0.5$ (as in our BL Lac sample), and are not classified as N-galaxies (whose color is affected by the light from the bright nucleus). After K-correcting the R-band data (the correction is negligible for the K band), and assuming $H-K = 0.22$ (Recilla-Cruz et al. 1990), we obtain $\langle R - H \rangle = 2.3 \pm 0.3$ mag, fully consistent with what we found for BL Lac host galaxies. It is true that the radio galaxies in Lilly & Longair (1982) are mostly FR II (high-luminosity) sources, while BL

Lac objects are most likely associated with FR I (low-luminosity) radio galaxies (Urry & Padovani 1995); however, there is growing evidence that FR I and FR II host galaxies have similar optical properties (Govoni et al. 2000; Scarpa & Urry 2000), so this is unlikely to distort the comparison.

Similar colors were reported by De Vries et al. (1998) for a different sample of radio galaxies of various morphological type, at $\langle z \rangle \sim 0.3$. They found $\langle R - H \rangle = 2.4$ mag (transformed from observed $\langle R - K \rangle = 3.0$ mag assuming $H-K=0.22$ mag and $K\text{-cor}=0.4$ mag for the R band; Fukugita et al. 1995), again consistent with the value for BL Lac hosts.

The R–H color depends on the age of the dominant stellar population in these galaxies. Due to the metallicity-age degeneracy, the limited information provided by a single color does not allow us to set a tight limit on the epoch of major star formation in these galaxies; however, our data are consistent with the expectation for a single, very old, coeval stellar population. In the bottom panel in Figure 3, the BL Lac host galaxy colors (now not K corrected) are shown to evolve similarly to stellar synthesis models with ages of formation of 4 and 10 Gyrs (solid lines). Similar results have been found for radio galaxies and non-active ellipticals (McCarthy 1993).

3.3. Radial Color Gradients

We derived R–H color profiles for the ten resolved sources combining NICMOS H-band data with the WFPC2 R-band data from Scarpa et al. (2000). Two of the ten (0502+675 and 1749+096) had such noisy profiles, due to the weakness of the host galaxy relative to the central point source, that we do not discuss them further. The eight remaining color profiles are shown in Figure 4. All but one host galaxy show a clear trend for R–H to decrease with increasing radius, that is, the galaxies become bluer in the outer regions. Table 3 gives for each object the slope of the color profile in the (R–H) - Log(r) plane.

Similar R–H color gradients for five BL Lac host galaxies were found by Kotilainen, Falomo & Scarpa et al. (1998a). Urry et al. (1999) reported V–I color profiles for six BL Lac objects based on HST WFPC2 data; because of the smaller wavelength baseline, any color gradients are weaker than in the present R–H color profiles, but the blue-ing trend is still visible in at least three host galaxies (1407+595, 2143-070, and 2254+074).

To better quantify this color gradient, we constructed an average R–H color profile, corresponding to the implicit assumption that all host galaxies have the same gradient (a likely oversimplification). We first normalized each profile by subtracting its average color, then averaged the eight normalized profiles, as shown in Figure 5. The error bars represent

the standard deviation of the data in each 1-kpc interval, and thus reflect the variation in color from object to object rather than measurement errors. The best-fit linear color gradient has slope $\Delta(R - H)/\Delta \log r = -0.2 \pm 0.1$ mag, consistent with previous reports ($\Delta(R - H)/\Delta \log r = -0.09 \pm 0.04$ mag for the five BL Lacs in Kotilainen, Falomo & Scarpa 1998a).

The present data offer strong evidence that BL Lac host galaxies become bluer away from the galaxy center. An immediate consequence (and a consistency check) is that the effective radius of the galaxy is a function of the selected filter. In Figure 6 we compare the best-fit effective radii derived from our HST data, i.e., NICMOS for the H band and WFPC2 for the R band. Even though errors are in some cases large, there is a clear tendency for the effective radius to be larger in the optical than in the infrared. This is clearly because as wavelength decreases a larger fraction of the total light lies in the external regions, i.e., the host galaxies are bluer on their outskirts.

Color gradients of the same sign have been found in several studies of normal elliptical galaxies (Borison et al. 1983; 1987; Cohen 1986; Peletier et al. 1990; Munn 1992). A value of $\Delta(V - K)/\Delta \log r = -0.16 \pm 0.18$ mag was found by Peletier et al. (1990) for a sample of 12 elliptical galaxies. Given the median redshift of our BL Lac sample ($z = 0.2$), our R-band profiles are roughly equivalent to their V-band data at $z = 0$; therefore, assuming H and K profiles are similar (since the red stars evolve only slowly), the V–K gradient measured by Peletier et al. is roughly equivalent to our R–H color gradient. The fact that our two values are similar therefore underscores the similarity of BL Lac host galaxies and normal ellipticals. Specifically, the stellar populations of active and non-active ellipticals must not be very different, not only in an integrated sense but differentially across the galaxy.

3.4. The Surface Brightness – Effective Radius Relation

Infrared observations map the bulk of the slowly evolving stellar populations of galaxies, and are therefore particularly appropriate for investigating luminosity and galaxy morphology. It is therefore useful to investigate the Kormendy relation between effective radius, r_e , and surface brightness at that radius, μ_e , in the H band. Plotting our best-fit values for μ_e and r_e for BL Lac host galaxies (Table 2) shows they follow the same well-defined correlation as non-active elliptical galaxies (Figure 7). The dispersion around the best linear fit is comparable to that found in the R band (Urry et al. 2000). Since the H-band fits are less well constrained (the uncertainties are larger; see Figure 6), the intrinsic correlation must be tighter, reinforcing that infrared observations are indeed optimal for

investigating the fundamental plane of ellipticals.

A linear fit to our data combined with those from Kotilainen, Falomo & Scarpa (1998a) gives $\mu_e = 3.8 \log r_e + 14.8 \text{ mag/arcsec}^2$, where r_e is in kiloparsecs. In the K band, for a sample of 59 normal elliptical galaxies, $\mu_e = 4.3 \log r_e + 14.3 \text{ mag/arcsec}^2$ has been found (Pahre et al. 1995, after conversion to our adopted cosmology). The agreement is very good considering the restricted range in r_e spanned by BL Lac hosts, which are all giant galaxies. Again, this result fully supports the picture in which all elliptical galaxies have the potential to experience a phase of nuclear activity.

4. Summary and Conclusions

The HST NICMOS Camera 2 was used to image 12 BL Lac objects in the H band. All sources were also observed previously with the HST WFPC2 in the R band. Ten of the 12 BL Lacs were clearly resolved in the H band, with the remaining two having luminous nuclei that probably swamp any surrounding galaxy light. From direct inspection of the NICMOS data (Figure 1), as well as from the R-band WFPC2 data (Falomo et al. 2000), we found no indication of distortion, asymmetry, or tails in the host galaxies, down to surface brightness $\mu_H \sim 18.5 \text{ mag/asec}^2$. To increase the signal-to-noise ratio and reach fainter structure, we extract for each source the azimuthally averaged radial profile, which is traced out to 3-4 arcsecs from the nucleus down to $\mu_H \sim 21 \text{ mag/asec}^2$ (Figure 2). This corresponds to 1-3 effective radii depending on galaxy distance and size.

The ten detected host galaxies are luminous ellipticals, with $r^{1/4}$ -law profiles. Their average K-corrected absolute H magnitude is $\langle M_H \rangle = -26.2$, with 1σ dispersion of 0.45 mag, about one magnitude brighter than an M* galaxy ($M_H^* = -25.0 \pm 0.3$ galaxy; Mobasher, Sharples & Ellis 1993), and their average effective radius is $\langle r_e \rangle = 10 \pm 5 \text{ kpc}$.

The average R–H color of the BL Lac host galaxies, $\langle R - H \rangle = 2.2 \pm 0.3 \text{ mag}$, is typical of normal ellipticals or radio galaxies, and indicates the dominant stellar population is more than a few gigayears old. Because of the high resolution of HST, we were able to detect color gradients in the majority of BL Lac host galaxies, such that their cores are redder than their external regions. From our color profiles, which probe a region extending from 0.2 to 1.5 effective radii, we measure an average color gradient of $\Delta(R - H)/\Delta \log r = -0.2 \pm 0.1 \text{ mag}$, again similar to those observed in elliptical galaxies (Peletier et al. 1990).

The infrared Kormendy relation for BL Lac host galaxies is indistinguishable from the same relation for normal elliptical galaxies. Thus they appear to occupy the same region of the fundamental plane as other ellipticals, including radio galaxies.

In every respect we could measure, the host galaxies of BL Lac objects appear to be normal ellipticals. Given the high precision of the HST data, our study was largely free of confusion from the bright nucleus. Had there been dust lanes or other morphological peculiarities beyond ~ 0.2 arcsec from the center, they would have been readily apparent. We conclude therefore that to first order, the host galaxy “knows” nothing about the active nucleus it harbors. This is in contrast to claims of a nuclear-host connection in more powerful AGN (McLure et al. 1999, McLeod & Rieke 1995). This result argues against AGN and galaxies being separate entities, and instead supports a picture in which all galaxies can be AGN but with a relatively low duty cycle. This implies all galaxies (at least, elliptical galaxies) have super-massive black holes at their centers, as indeed appears to be the case in many nearby ellipticals (Richstone et al. 1998, van der Marel 1999).

Because active galaxies are often observed in clusters, it has been proposed that galaxy mergers are responsible for initiating the nuclear activity. In the HST images of BL Lac objects we do not see any of the morphological peculiarities (e.g., tails, dust lanes) or unusual stellar content which might be expected following a merger. A possibility is that in the vast majority of cases the nuclear activity is triggered by merge of a companion galaxy so small that the global properties of the main galaxy remain unchanged. However, better constraints on this hypothesis would have been possible were we to obtain additional images in a bluer filter. In any case, the present work strongly supports a picture in which all galaxies have the potential to be active. This in turn suggests the formation and evolution of galaxies occurred hand in hand with the growth of super-massive black holes at their centers.

Support for this work was provided by NASA through grant number GO-07893.01-96A from the Space Telescope Science Institute, which is operated by AURA, Inc., under NASA contract NAS 5-26555. This research made use of NASA’s Astrophysics Data System Abstract Service (ADS).

References

- Abraham R.G., McHardy I.M. & Crawford C.S. 1991, MNRAS 252, 482
- Boroson T.A., Thompson I.B. & Sackett P.A. 1983, AJ 88, 1707
- Boroson T.A. & Thompson I.B. 1987, AJ 93, 33
- Cohen J.G. 1986, AJ 92, 1039
- de Vries W.H., O’Dea C.P., Baum S.A. & Perlman E. 1998, ApJ 503, 156
- Falomo R. & Kotilainen J.K. 1999, A&A 352, 85

- Falomo R., Urry C.M., Pesce J.E., Scarpa R., Giavalisco M. & Treves A. 1997, *ApJ* 476, 113
- Fukugita M., Shimasaku K. & Ichikawa T. 1995, *PASP* 107, 945
- Govoni F., Falomo R., Fasano G. & Scarpa R. 2000, *A&A* 353, 507
- Jannuzi B.T., Yanny B. & Impey C. 1997, *ApJ* 491, 146
- Kotilainen J.K., Falomo R. & Scarpa R. 1998a, *A&A* 336, 479
- Kotilainen J.K., Falomo R. & Scarpa R. 1998b, *A&A* 332, 503
- Krist, J. 1995, in *Astronomical Data Analysis, Software and Systems IV*, eds. R. Shaw et al., (San Francisco: Astr. Soc. Pac.), p. 349
- Lilly S.J. & Longair M.S. 1982, *MNRAS* 199, 1053
- McCarthy P. 1993, *PASP* 105, 1051
- McLeod K.K. & Rieke G.H. 1995, *AJ* 109, 1979
- McLure R.J., Kukula M.J., Dunlop J.S., Baum S.A., O’Dea C.P. & Hughes D.H. 1999, *MNRAS* 308, 377
- Mobasher B., Sharples R. M. & Ellis R. S. 1993, *MNRAS* 263, 560
- Munn J.A. 1992, *ApJ* 399, 444
- Pahre M.A., Djorgovski S.G. & De Carvalho R.R. 1995, *ApJL* 435, 17
- Peletier R.F., Valentijn E.A. & Jameson R.F. 1990, *A&A* 233, 62
- Recillas-Cruz E., Carrasco L., Serrano A. & Cruz-Gonzales I. 1990, *A&A* 229, 64
- Richstone, D., et al. 1998, *Nature* 395, 14
- Scarpa R. & Urry C. M. 2000, in preparation
- Scarpa R., Urry C. M., Falomo R., Pesce J. E. & Treves A. 2000, *ApJS*, 532, 740
- Sillanpää A., Takalo L.O., Nilsson K., Pursimo T. & Pietilä 1998, in *BL Lac Phenomenon*, A.S.P. Conf. Ser., Vol. 159, ed. L.T. Takalo and A. Sillanpää, p. 395
- Stickel M., Fried J.W., & Kühr H. 1993, *A&AS* 98, 393
- Urry C.M. & Padovani P. 1995, *PASP* 107, 803
- Urry C.M., Scarpa R., O’Dowd M., Falomo R., Pesce J.E., Treves A. & Giavalisco M. 1999, *ApJ* 512, 88

- Urry C.M., Scarpa R., O’Dowd M., Falomo R., Pesce J.E., & Treves A. 2000, ApJ, 532, 861
- Urry, C.M. 1999 Astroparticle Physics 11, 159
- Ulrich M.-H. 1989, in “BL Lac objects’, ed. L. Maraschi, T. Maccacaro and M.-H. Ulrich (Springer, Berlin), p. 92
- van der Marel, R. 1999, AJ 117, 744
- Wurtz R., Stocke J.T. & Yee H.K.C. 1996, ApJS 103, 109
- Yanny B., Jannuzi B.T. & Impey C. 1997, ApJ 484, L113

Figure Caption.

Figure 1: Contour plots from the central 7.5×7.5 arcsec regions of the combined NICMOS F160W images of all 12 BL Lac objects. Isophotes are spaced by 0.5 magnitudes and the surface brightness of the fainter is given in each panel (in mag/arcsec²). To improve the visibility of low surface brightness structure, the images have been smoothed using a Gaussian filter with width 0.0375 arcsec. The arrow points north. The host galaxies are resolved in 10 of 12 cases, the two unresolved BL Lacs being 0454+884 and 0851+302. Whatever structure is visible in the latter two images is due to the point spread function, as is the bridge that appears to connect 0607+710 to the nearby star.

Figure 2: Azimuthally averaged surface brightness radial profile (*points with error bars*), and the best-fit point source plus de Vaucouleurs model (or only the point source for unresolved sources). *Dotted line:* the point source model (PSF). *Dashed line:* de Vaucouleurs model convolved with the PSF. *Solid line:* sum of the two model components. When not visible, the dashed line is superimposed on the solid line, and the solid line is covered by the observed points. The PSF model works very well, as evidenced by how it fits the profiles of the unresolved BL Lacs (0454+884 and 0851+202), out to more than 3 arcsec. Nine of the remaining 10 objects have strong excess emission above the PSF; the tenth, 1749+096, has a host galaxy only marginally detected above the PSF but at the level expected given the HST R-band detection.

Figure 3: BL Lac host galaxy R–H color as a function of redshift, showing their similarity to normal ellipticals with old stellar populations. *Solid squares:* our HST data; *open squares:* ground-based data from Kotilainen, Falomo & Scarpa (1998a). **Upper panel:** Rest-frame colors, with both extinction and K corrections applied. The horizontal line at R–H=2.3 mag is the average color observed for normal elliptical galaxies (Kotilainen Falomo & Scarpa 1998a). **Lower panel:** Observed colors (i.e., extinction- but not K-corrected) of BL Lac host galaxies compared to the expected colors for coeval stellar populations with age 10 Gyrs (*upper line*) and 4 Gyrs (*lower line*).

Figure 4: R–H color profiles of BL Lac host galaxies. Two objects, 0502+675 and 1749+096, are omitted because the signal-to-noise ratios for their host galaxies are very low. With the exception of 0229+200, the host galaxies become significantly bluer in their outer regions, as observed in normal elliptical galaxies (Peletier et al. 1990).

Figure 5: Average color profile for the 8 well-resolved sources, derived from profiles in Figure 4. Profiles were combined after first subtracting their average color, then computing the weighed average of the points on intervals of 1 kpc. The formal statistical error on each point is smaller than the size of the symbol, while the intrinsic dispersion of the points

in each bin is shown at the top-left corner of the figure. The best fit slope (*solid line*) is $\Delta(R - H)/\Delta \log r = -0.2 \pm 0.1$ mag.

Figure 6: Comparison of effective radii derived from WFPC2 (R-band) and NICMOS (H-band) images. The solid line is the locus of an exact match between the two measures, while the dashed line is a linear fit to the data. This shows that the R-band effective radius is larger than the H-band one, reflecting the fact that the host galaxies become systematically bluer in their outer regions. Two objects show an opposite behavior; for 1749+096, the measurement has large uncertainties, while for 0229+200 the lack of color gradient may be real.

Figure 7: The H-band $\mu_e - r_e$ relation for BL Lac host galaxies. *Solid squares:* our HST data; *open squares:* ground-based data from Kotilainen, Falomo & Scarpa (1998a). *Solid line:* linear fit to the data; *dashed line:* best-fit relation for a sample of 59 normal ellipticals reported by Pahre et al. (1995).

Table 1. **Journal of the Observations**

BL Lac Object	Sample/ Name	Date Obs.	Exp.Time ^(a) (sec)
0229+200	1ES	06-Jan-98	320
0454+844	S5	26-Sep-98	1920
0502+675	1ES	04-May-98	1428
0607+710	MS	03-Jun-98	896
0706+591	EXO	20-Apr-98	352
0851+202	1Jy/OJ287	18-Oct-98	896
1212+078	1ES	10-Mar-98	352
1407+595	MS	20-Sep-98	1408
1418+546	PG	25-Sep-98	352
1749+096	PKS	09-Aug-98	1024
2143+070	EMSS	09-Nov-98	960
2356-309	HEAO-A3	14-Oct-98	831

^(a)Total exposure time, i.e., sum of exposure times for all images.

Table 2. Host Galaxy Properties

BL Lac object	z	$A_H^{(a)}$	K Corr. H band	$m_H^{(b)}$ (tot)	$m_H^{(c)}$ (PSF)	$m_H^{(d)}$ (host)	$\mu_e^{(e)}$	$r_e^{(f)}$ (arcsec)	$M_H^{(g)}$ (PSF)	$M_H^{(h)}$ (host)	r_e (kpc)
0229+200	0.139	0.13	0.01	13.56	16.0 ± 0.2	12.8 ± 0.1	18.38	3.8 ± 0.6	-23.89	-27.1	12 ± 2
0454+844	>1.34	0.09	...	16.60	-29.13
0502+675	0.314	0.16	0.03	18.56	18.7 ± 0.2	15.7 ± 0.3	16.20	0.5 ± 0.2	-23.16	-26.1	3.0 ± 1.2
0607+710	0.267	0.13	0.02	15.05	16.8 ± 0.2	14.8 ± 0.1	18.40	1.9 ± 0.3	-24.63	-26.6	10.5 ± 1.6
0706+591	0.125	0.08	0.01	13.91	15.7 ± 0.1	13.4 ± 0.1	18.34	2.7 ± 0.2	-23.89	-26.2	8.2 ± 0.6
0851+202	0.306	0.05	0.03	16.60	-25.08
1212+078	0.136	0.02	0.01	13.92	15.8 ± 0.2	13.6 ± 0.1	17.91	2 ± 0.6	-23.93	-26.1	6.5 ± 1.9
1407+595	0.495	0.02	0.11	16.05	17.0 ± 0.2	16.1 ± 0.2	18.76	1.7 ± 0.3	-25.87	-26.9	13.7 ± 2.4
1418+546	0.152	0.01	0.01	12.74	13.0 ± 0.1	13.7 ± 0.2	18.84	3 ± 0.3	-26.97	-26.3	10.7 ± 1.1
1749+096	0.320	0.06	0.03	13.15	13.2 ± 0.1	15.3 ± 0.3	19.98	3.3 ± 1.5	-28.60	-26.5	20 ± 9
2143+070	0.237	0.07	0.02	15.22	16.2 ± 0.2	15.3 ± 0.2	18.55	1.5 ± 0.4	-24.88	-25.7	7.6 ± 2.0
2356-309	0.165	0.02	0.01	14.41	15.2 ± 0.1	14.7 ± 0.1	18.54	1.7 ± 0.2	-24.97	-25.5	6.5 ± 0.8
Median	0.237					14.75				-26.2	9.4

^(a)Interstellar extinction in magnitudes, derived assuming $A_H = 0.25A_R$

^(b)Observed H-band magnitude of the BL Lac source, integrated to the last point of the radial profile shown in Figure 2. Values in this column are neither extinction nor k corrected. Systematic+statistical errors for these values are $\sim 10\%$.

^(c)H-band magnitude of the point source from the best-fit PSF, neither extinction nor k corrected.

^(d)H-band total magnitude of the host galaxy, obtained integrating the best-fit de Vaucouleurs law to infinite radius. No extinction nor k correction applied.

^(e)H-band surface brightness of the host galaxy at the effective radius, r_e , in mag/arcsec². Values include extinction correction, K-correction, and cosmological dimming.

^(f)Effective radius of the best-fit de Vaucouleurs law, i.e., radius which encloses half the total light.

^(g)Absolute magnitude of the central point sources, computed for $H_0 = 50$ km/s/Mpc, $q_0 = 0$, and corrected for interstellar extinction. K-correction is assumed to be zero because BL Lac nuclei have power law spectra with spectral index ~ -1 .

^(h)Absolute total magnitudes of the host galaxy, extinction and k-corrected.

Table 3. **Host Galaxy Colors**

Object	R–H ^(a) (mag)	Δ (R–H)/ $\Delta \log(r)$ (mag)
0229+200	2.5 ± 0.1	+0.0
0502+675	2.3 ± 0.3	...
0607+710	2.3 ± 0.1	–0.3
0706+591	2.2 ± 0.1	–0.3
1212+078	2.2 ± 0.1	–0.6
1407+595	2.1 ± 0.2	–0.8
1418+546	2.2 ± 0.2	–0.5
1749+096	2.9 ± 1.3	...
2143+070	1.7 ± 0.2	–0.6
2356-309	2.2 ± 0.1	–0.3
Mean Profile		–0.2

^(a)Integrated rest frame R–H color, K-corrected and corrected for extinction. Color gradients are expressed in magnitudes per decade, i.e., it is the variation of color for $\Delta \log(r) = 1$.

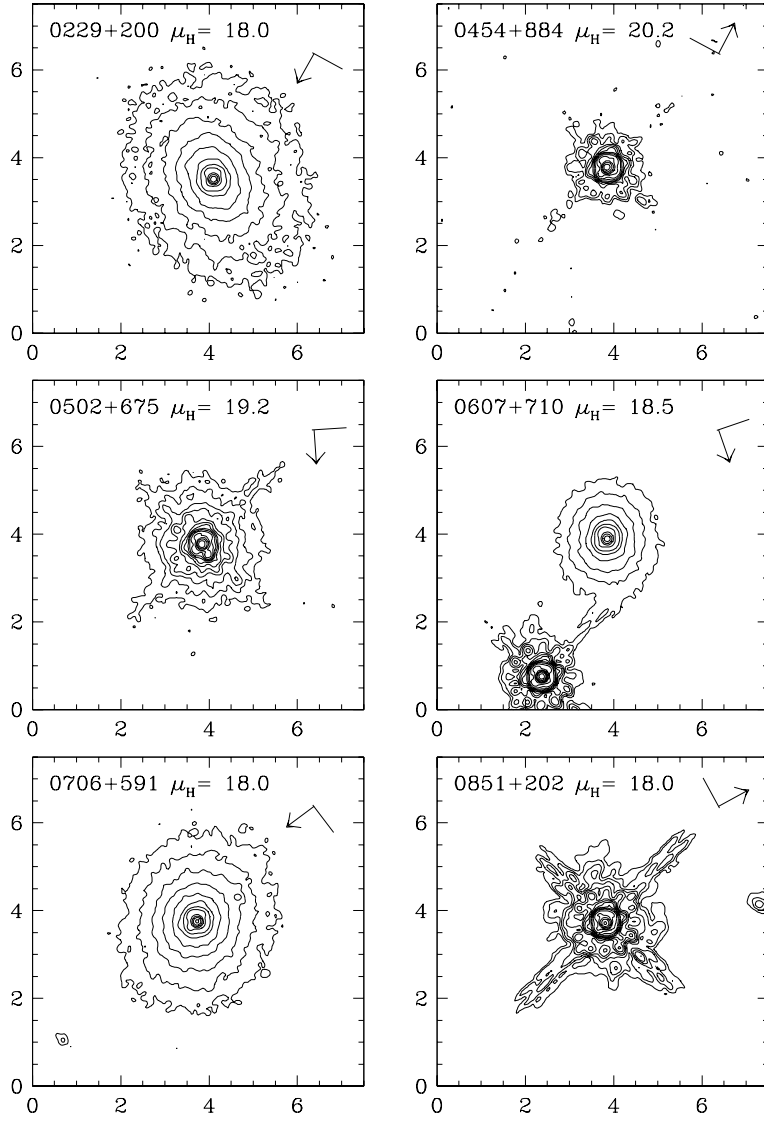
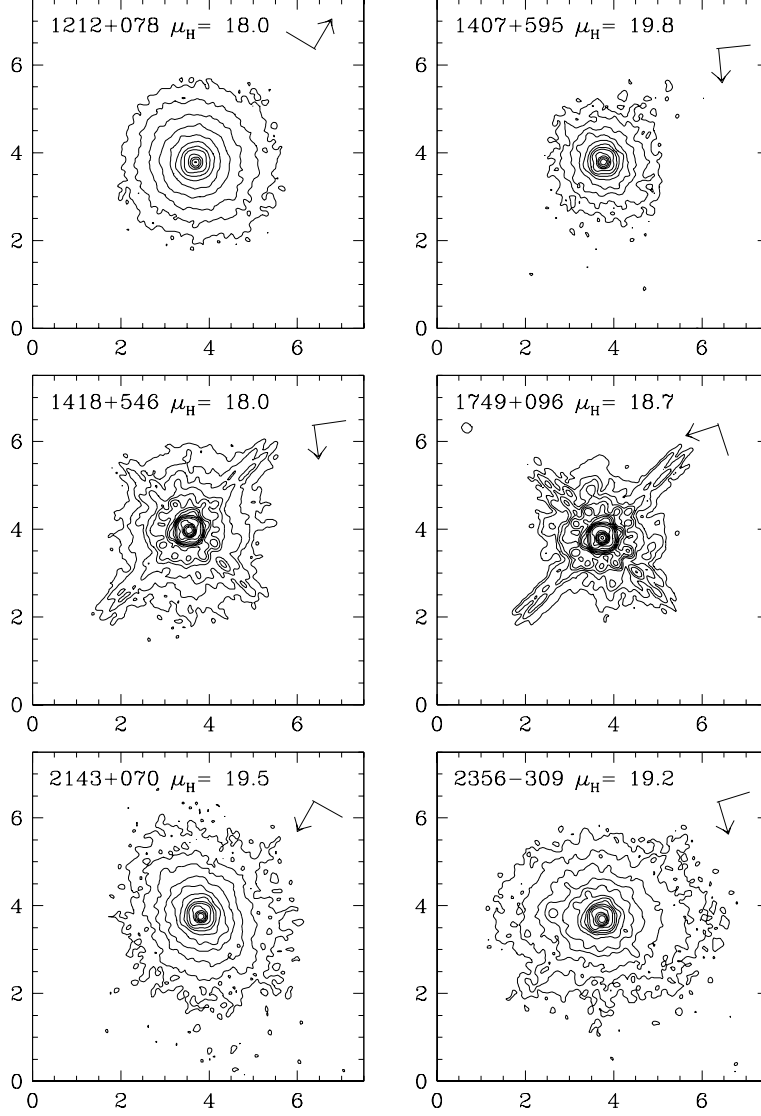


Fig. 1.—



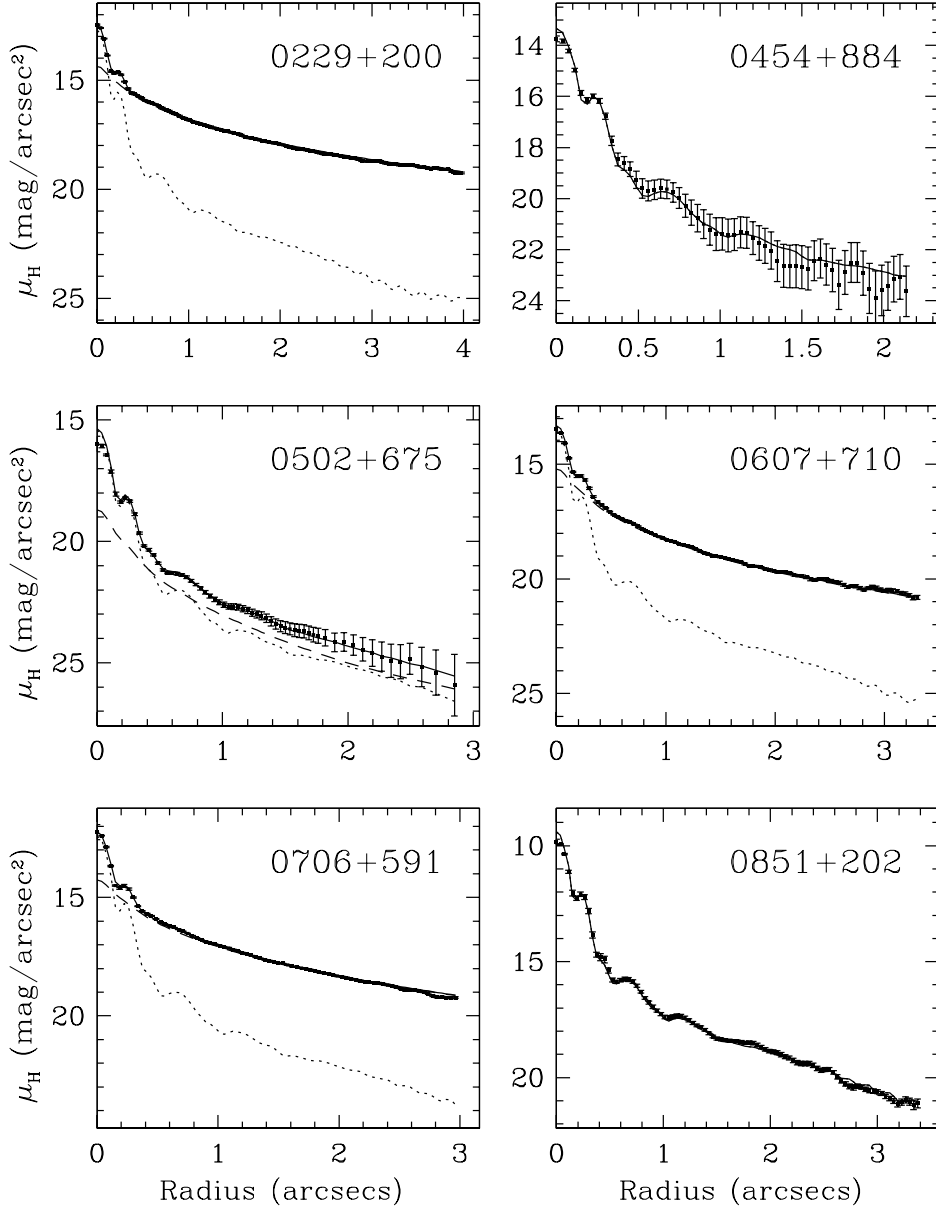
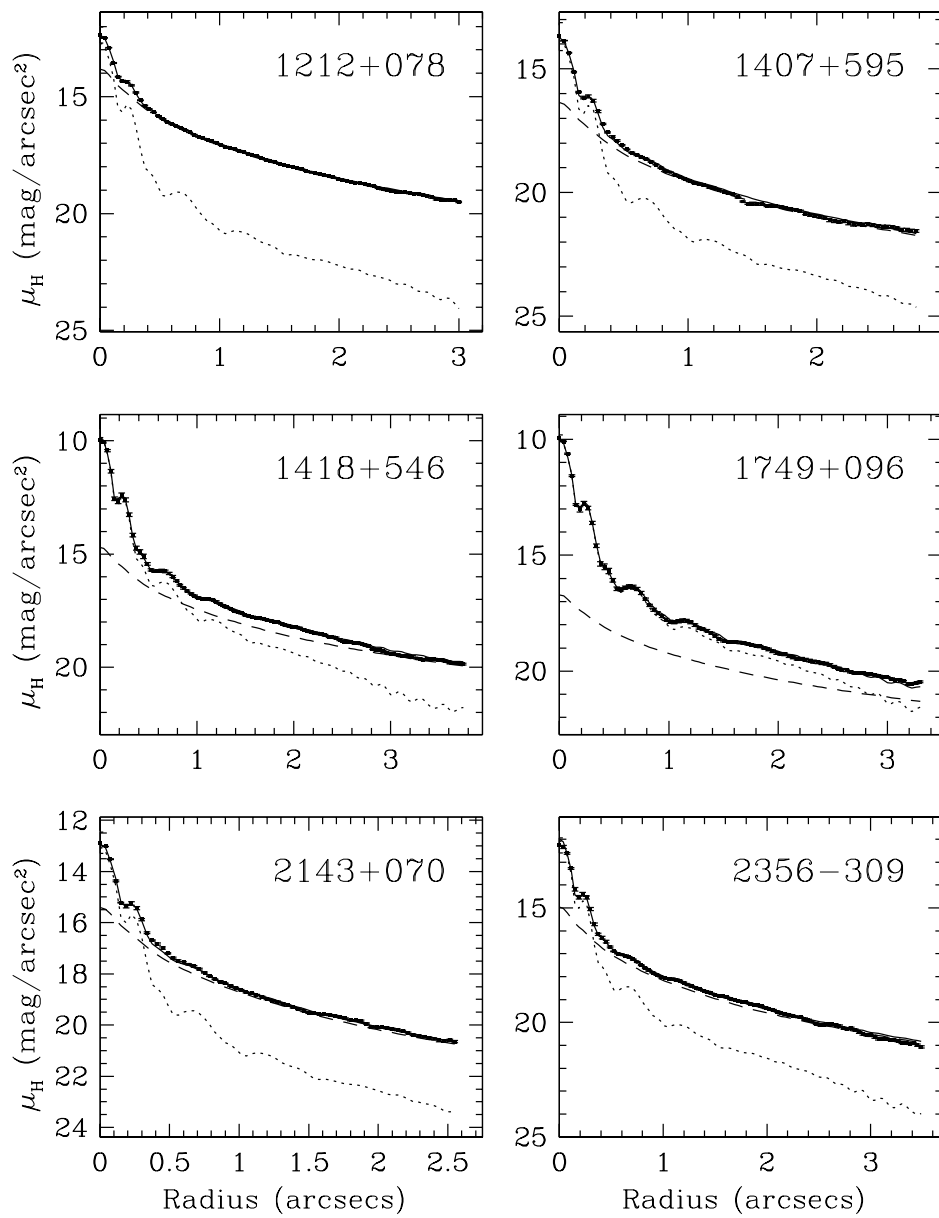


Fig. 2.—



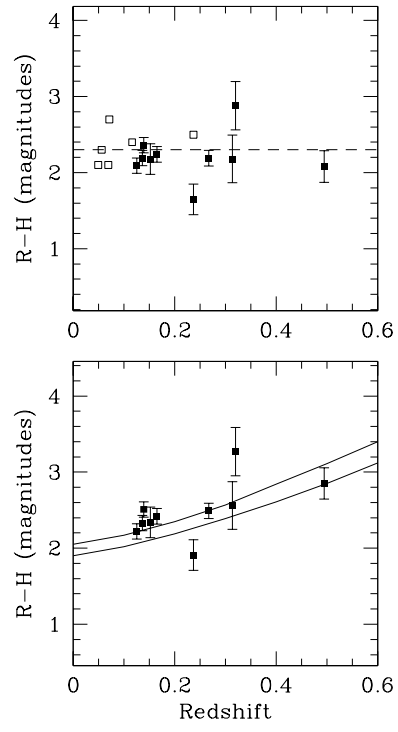


Fig. 3.—

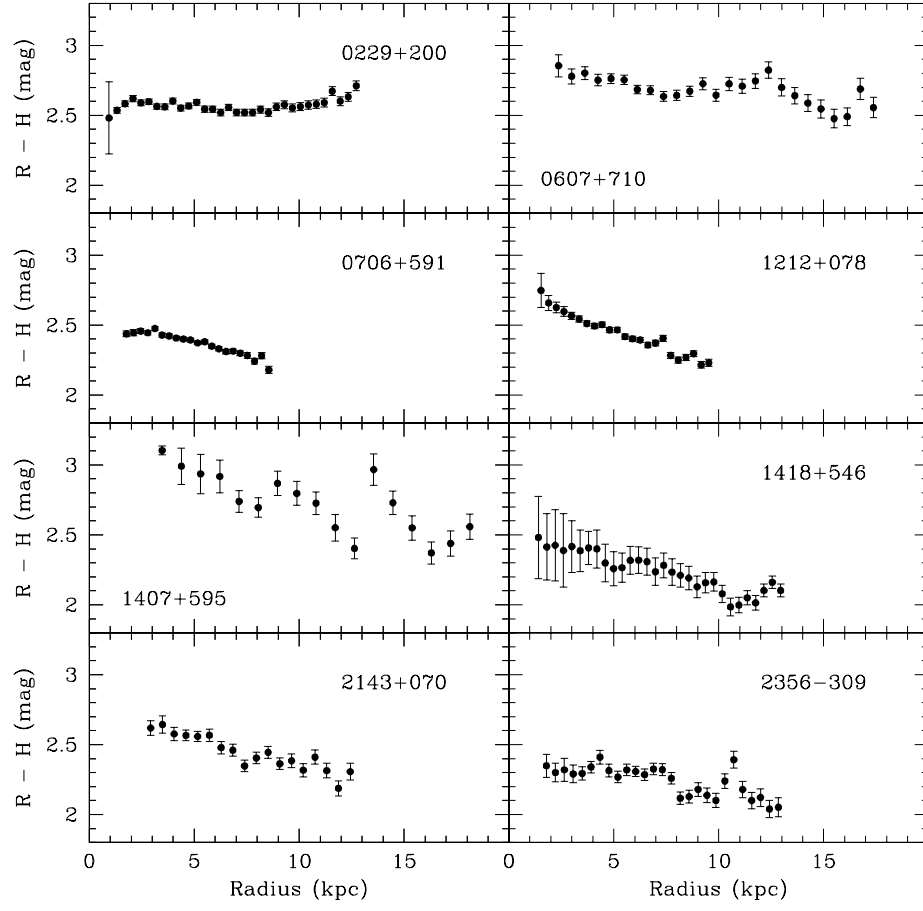


Fig. 4.—

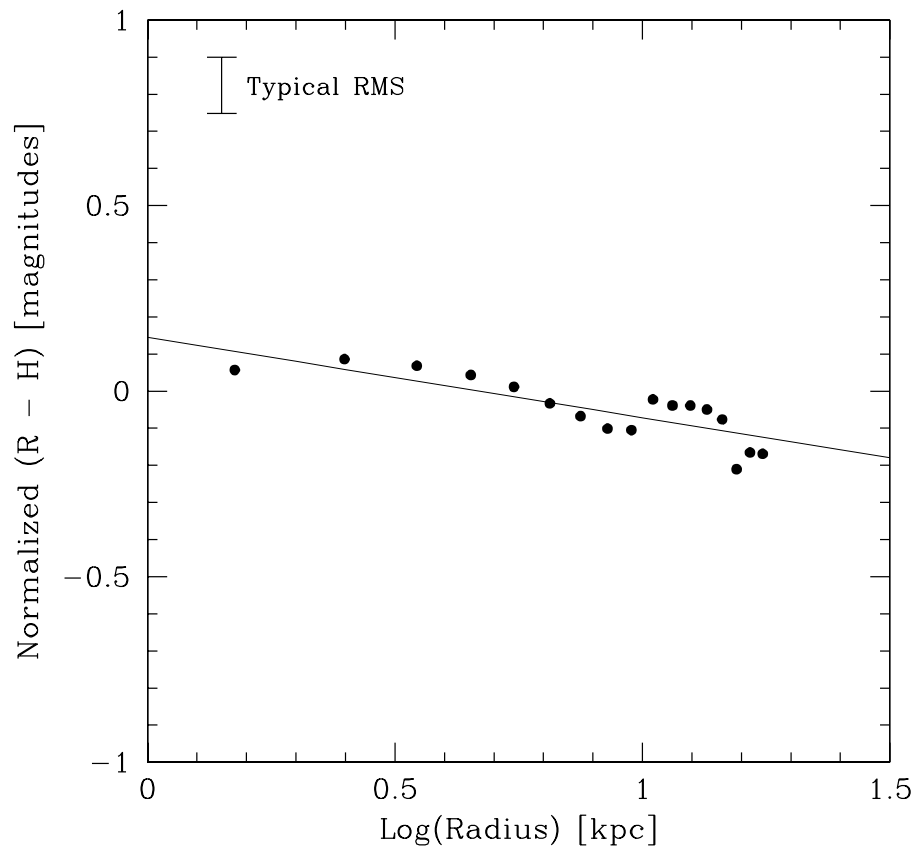


Fig. 5.—

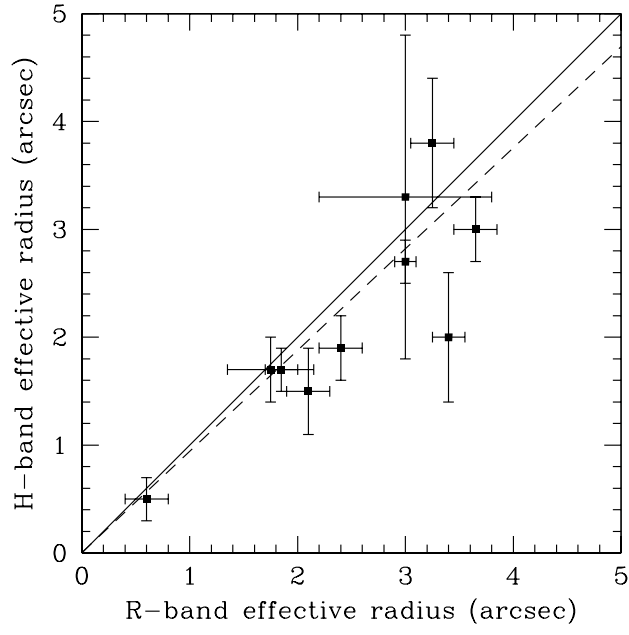


Fig. 6.—

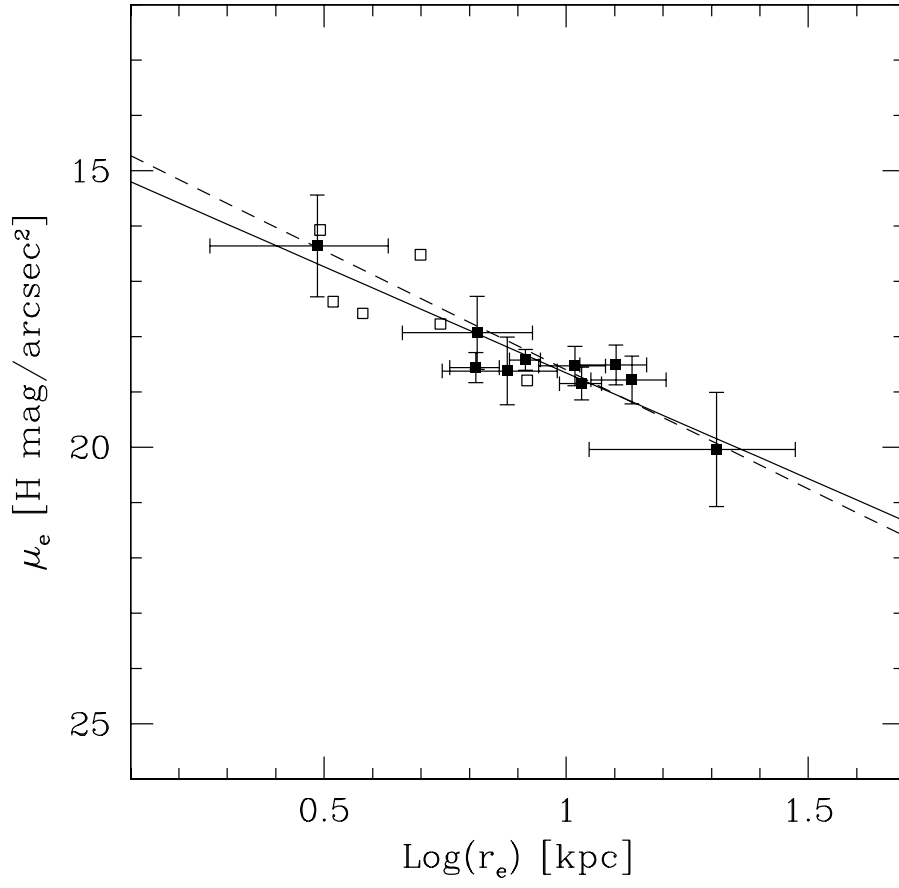


Fig. 7.—